International Conference "Water, Environment, Energy and Society" (WEES–2009)
New Delhi, 12–16 January 2009

The Influence of the Land Surface on Hydrometeorology and Ecology: New Advances from Modeling and Satellite Remote Sensing

Seungbum Hong[1] and Venkat Lakshmi[2]
Department of Geological Sciences
University of South Carolina, Columbia, SC 29201
E-mail: [1]shong@geol.sc.edu; [2]venkat-lakshmi@sc.edu

Eric E. Small
Department of Geological Sciences
University of Colorado, Boulder, CO 80309
E-mail: Eric.Small@colorado.edu

Fei Chen
Research Application Lab
National Center for Atmospheric Research, Boulder, CO 80307
E-mail: feichen@ucar.edu

ABSTRACT: The importance of land surface processes has long been recognized in hydrometeorology and ecology for they play a key role in climate and weather modeling. However their quantification has been challenging due to the complex nature of the land surface amongst various other reasons. One of the difficult parts in the quantification is the effect of vegetation which are related to land surface processes such soil moisture variation and to atmospheric conditions such as radiation. This study addresses various relational investigations among vegetation properties such as Normalized Difference Vegetation Index (NDVI), Leaf Area Index (LAI), Surface Temperature (TSK) and Vegetation Water Content (VegWC) derived from satellite sensors such as Moderate Resolution Imaging Spectroradiometer (MODIS) and EOS Advanced Microwave Scanning Radiometer (AMSR-E). The study provides general information about a physiological behavior of vegetation for various environmental conditions. Second, using a coupled mesoscale/land surface model, we examined the effects of vegetation and its relationship with soil moisture on the simulated land-atmospheric interactions through the model sensitivity tests. The Weather Research and Forecasting (WRF) model was selected for this study and the Noah Land Surface Model (Noah LSM) implemented in the WRF model was used for the model coupled system. This coupled model was tested through two parameterization methods for vegetation fraction using MODIS data and through model initialization of soil moisture from High Resolution Land Data Assimilation System (HRLDAS). Then, this study evaluates the model improvements for each simulation method.

INTRODUCTION

Influences of land surface processes on hydro-meteorology are presented in the interactions between land and atmosphere and the studies of the land and atmospheric interactions have provided critical information for numerical weather and climate modeling. The land and atmospheric interactions are generally regarded as water vapor cycle in near surface which is closely related to surface moisture status. This surface moisture status varies with land surface processes, effecting on atmospheric features and vice versa. For example, the variations of surface energy and moisture fluxes by soil and vegetation surface are strongly related to thunderstorm formation (Pielke, 2001). Meanwhile, climate and meteorological variations impact land surface characteristics such as vegetation distribution, energy balance and watershed hydrology (e.g., Small and Kurc, 2003; Weiss *et al.*, 2004). The hydrological properties of soil and vegetation play a very important role in quantification of the surface moisture status. For example, the soil type with varying hydraulic conductivities determine the moisture status of soil surface and vegetation properties such as canopy height, leaf amount and root zone determines vegetation transpiration. Soil and vegetation also directly impact on each other. For example, properties of the root zone such as its depth and width have an impact on vertical moisture distribution in soil layers (Kleidon & Heimann, 1998; Pielke, 2001). One of the recent technologies to

implement the land and atmospheric interaction into numerical modeling is the coupling system between a mesosacle and land surface model. For over a decade, this model coupling system has been developed to provide improved simulations with various field projects. Among the quantifications of land surface properties which determine surface moisture variation, vegetation behaviors has been the most difficult aspect because of their complex relationships with atmosphere as well as other land surface processes. It has been challenged to quantify the hydrological properties of vegetation for several decades and that still plays very important role to improve current forecasting models.

In order to evaluate the contribution of vegetation to the land and atmospheric interactions, this study addresses investigations of the relationships among vegetation properties, using satellite-derived data: Normalized Difference Vegetation Index (NDVI), Leaf Area Index (LAI), Vegetation Water Content (VegWC) and skin surface temperature (Ts). The main purpose of this is to evaluate the meteorological effect of satellite derived VegWC and the prospect for its application to numerical forecasting models through the following relational analyses with the other variables: (1) relationship between LAI and VegWC, (2) between NDVI and VegWC and (3) between NDVI, Ts and VegWC. For these analyses, three climatically characteristic regions in North America are selected: semi-arid, intermediate and humid regions. Next, this study provides investigations of the land surface and atmospheric interactions from simulation results of a coupled mesoscale/land surface model. The main purposes of these investigations are to evaluate the simulation accuracy from the model physics related to the surface moisture status and the model sensitivity to the moisture status variation in soil and vegetation surfaces. For the model accuracy test, some land surface variables and parameters in several grid points of the study area are replaced using field measurement data and vegetation parameterization and soil moisture data assimilation are performed for the model sensitivity tests. In both studies, the statistical analyses and time series comparisons with the field measurements are provided to validate the model simulations.

DATA AND METHOD

Study Areas

Three regions have been selected to examine the spatial variations of the land surface variables (Figure 1); (1) the North American Monsoon System (NAMS) region; (2) South Great Plains (SGP) region and (3) Little River Watershed in Tifton, Georgia. The geographic latitude and longitude of their center points are 33.5 N and 107.5 W, 36.5 N and 100.0 W and 32.4 N and 84.0 W, respectively. The NAMS region has been the focus of numerous studies on the interactions between meteorology, vegetation and land surface fluxes (Kurc and Small, 2004; Weiss *et al.*, 2004). For the comparisons of the climate changes in NAMS region to other regions, the International H_2O Project (IHOP_2002) has been undertaken since 2002 (Weckwerth *et al.*, 2004) in SGP region. The Little River Watershed region around Tifton, Georgia as one of the highly vegetated regions in east coast areas has been a subject for soil moisture research. This region has a humid climate and denser vegetation than the NAMS and SGP regions. Because of the short-term but very frequent rainfall events in summer, it has large inundated areas with mixed forests (Bosch *et al.*, 1999). Satellite data have been processed in equal-sized areas (500 km × 500 km) for those study regions and they are referred to as follows: NAMS, IHOP and Tifton, GA. Figure 1 shows typical climatic trends of the three regions. The NAMS region is relatively dry

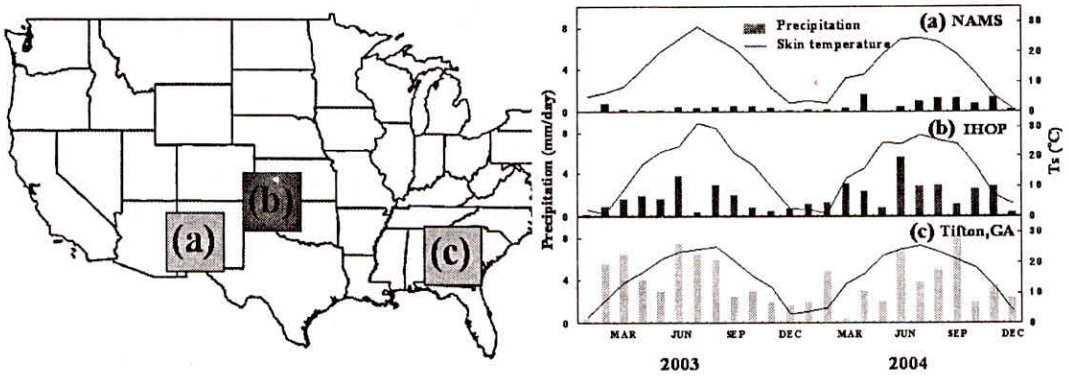

Fig. 1: Three selected study regions and the climograph of each region with precipitation and surface temperature (data from www.cdc.noaa.gov)

with relatively low vegetation amount. Major types of vegetation in this region are shrublands with limited grasslands and crops. The IHOP region, in contrast, shows relatively more humid climate with more vegetation which is grasslands, crops and limited trees. Tifton, GA is highly vegetated with mixed forest (*e.g.* pines and hardwoods) and crops (*e.g.* peanuts and cotton), showing wet and humid climate with highly frequent rainfalls. Of the three study regions, IHOP region was especially selected to the coupled model tests due to the availability of ground observations.

Satellite Data

We obtained two different satellite data: Moderate Resolution Imaging Spectroradiometer (MODIS) and Advanced Microwave Scanning Radiometer for Earth Observing System (AMSR-E). MODIS flies onboard the Terra and Aqua satellite platforms, which were launched on December 18, 1999 and on May 4, 2002, respectively and only Terra MODIS data were utilized for this study. The algorithms of the MODIS land data are available at the MODIS website (http://modis.gsfc.nasa.gov) and we downloaded the land data, surface reflectance, NDVI, Ts and LAI from the Land Processes Distributed Active Archive Center (LPDAAC) website (http://edcdacc.usgs.gov) for this study. The AMSR-E instrument on the NASA EOS Aqua satellite provides global passive microwave measurements of terrestrial, oceanic and atmospheric variables for the investigation of global water and energy cycles (Njoku *et al.*, 2003; Shibata *et al.*, 2003). The AMSR-E observed brightness temperatures at the 6, 10 and 18 GHz are used in conjunction with a radiative transfer model to simultaneously retrieve the surface soil moisture, Ts and VegWC. The radiative transfer model is run in an iterative fashion and these three variables are adjusted until the simulated brightness temperatures at the three channels match closely with the AMSR-E observed brightness temperatures at the same location (Njoku *et al.*, 2003). The algorithm derived VegWC, soil moisture and Ts global daily data is stored at the National Snow and Ice Data Center (NSIDC) website (http://www.nsidc.org/data/amsre). We acquired VegWC data from this web site for our study regions and the time period of interest.

NDVI is a biophysical parameter that quantifies the photosynthetic activity of vegetation by observing the 'greenness' of the vegetation which is related to the chlorophyll abundance and energy absorption (Tucker, 1979; Myneni *et al.*, 1995). NDVI has been widely used for various studies on dynamic land surface changes such as deforestation and drought and as an important variable to model simulations such as land surface hydrology and land-atmosphere interactions.

NDVI is derived using the normalized ratio of the red and near infra-red surface reflectances (Tucker, 1979). MODIS also provides surface temperature (Ts), which is derived from thermal infrared data (Justice *et al.*, 1998; Wan and Li, 1997). Surface temperature is an important variable linking evapotranspiration (ET) to soil moisture availability. Lower soil moisture and ET yield higher surface temperature and greater sensible heating of the atmosphere (Small and Kurc, 2003). We used day values (1030am equatorial overpass) from the daily 1 km resolution Ts data of MODIS. LAI is defined as the one sided green leaf area per unit ground area in broadleaf canopies and as the projected needle leaf area in coniferous canopies (Myneni *et al.*, 2002). LAI affects the fluxes of energy, mass and momentum between the surface and the planetary boundary layer (Justice *et al.*, 1998). The MODIS LAI is derived from a vegetation land cover classification and MODIS surface reflectance (Justice *et al.*, 1998; Myneni *et al.*, 1997). The algorithm uses 6 biome types which represent architecture of an individual tree and transmittance of vegetation elements.

From AMSR-E, VegWC is retrieved from a radiative transfer model in which vegetation opacity is used to derive VegWC at low frequency (Njoku and Li, 1999). The AMSR-E VegWC possibly has biased data values particularly on water bodies and bare soil areas. AMSR-E VegWC is derived from surface roughness parameter incorporating effects both of vegetation and roughness (Njoku *et al.*, 2003; Njoku and Chan, 2005). Since roughness and vegetation have similar trends in their effects on the normalized polarization differences, the algorithm assumes the surface roughness parameter as VegWC (Njoku and Chan, 2005). However, this assumption is acceptable only for smooth surface with vegetation. For example, a non-zero VegWC value in a desert area is only due to surface roughness. To avoid this error, we selected study regions primarily not including any water bodies and bare soil areas and assumed that the selected regions have smooth vegetated surface and are not affected by any surface roughness other than vegetation. In the case of irrigated/flooded land surfaces, the soil moisture retrieved from the AMSR-E brightness temperature will show saturated values but the retrieval of VegWC will be unaffected.

Additionally, we created a new satellite variable using VegWC and LAI. Ceccato *et al.* (2001, 2002b) found that NDVI and VegWC did not co-vary in a

simple fashion, which may be attributed to differences between biomes in contrasting climatic regimes. A decrease in chlorophyll content, which is considered to reflect a decrease in NDVI, does not directly indicate a decrease in VegWC and *vice versa*. Larger vegetation structures are likely to have higher vegetation water content. In order to examine the indirect relationships between the variables, we made a new variable, the Normalized Vegetation Water Content (NVegWC) defined as VegWC per unit plant leaf area (the ratio of VegWC and LAI), which is linked with the leaf water conservation mechanism. It is a very useful descriptor especially when we compare vegetation across biomes which may have different species of vegetation with different leaf area indices and vegetation water contents. Our intent with calculating NVegWC was to facilitate a biome-to-biome comparison of vegetation water content and its relationship with other variables such as NDVI.

Data Processing for Satellite Variable Comparisons

All MODIS data sets used in this study have a 1 km spatial resolution while AMSR-E data is at 25 km with a different map projection type. Thus, in this study all data sets had to be resampled to be consistent with each other. All 1 km MODIS data were converted to 25 km resolution as AMSR-E data and the different spatial projection types between MODIS and AMSR-E were changed to the same AMSR-E geographical projection. The sinusoidal projection of MODIS data sets was converted into the AMSR-E geographical projection by nearest neighbor method with the help of MODIS re-projection tool (developed by NASA) and 25 pixels of 1 km MODIS data were aggregated and averaged to compose the 25 km spatial resolution. Then each data set has been averaged for the 3-month summer season (June 9th to September 12th). When data sets are re-sampled, errors are inevitable. To minimize this error, we removed the cloud-contaminated MODIS data pixels based on the data retrieval quality information provided for every pixel and then analyzed the standard deviation for each process. Linear and non-linear regression analyses were conducted to find correlations between the variables and one of the variables was color-coded into the two-variable relationship. The value of NVegWC was color-coded in the Ts-NDVI relationship.

Model Description

We used the coupled Noah/WRF model for the model tests. This model was originally designed by Chen and Dudhia (2001) with the 5th generation Mesoscale Model (MM5) and the Oregon State University land surface model (OSULSM or later Noah LSM). The MM5 model has been jointly developed by the Pennsylvania State University and the National Center for Atmospheric Research (NCAR). This model has been widely used for numerical weather prediction, air quality studies and hydrological studies. The motivation of the coupling of the MM5 and the Noah LSM was the existing simple LSM in MM5 which was not compatible to the complexity of physical processes of land surface. The Weather Research and Forecasting (WRF) model, a successor of the MM5 with the model coupling technique, is a mesoscale model for numerical weather forecasting and data assimilation system (Skamarock *et al.*, 2005). Maintained and supported as a community model to facilitate wide use for researching and teaching in the university community, the WRF model is suitable for use in a broad spectrum of applications across scales ranging from meters to thousands of kilometers. This includes research and operational numerical weather prediction, data assimilation and parameterized-physics research, downscaling climate simulations, driving air quality models and etc., and also offers numerous physics options such as microphysics, surface physics, atmospheric radiation physics and planetary boundary layer physics.

The Noah LSM used for this model-coupling approach was originally developed by Pan and Mahrt (1987). Its hydrological physics is based on the diurnally dependent Penman potential evaporation approach (Mahrt and Ek, 1984), the multi-layer soil model (Mahrt and Pan, 1984) and the primitive canopy model (Pan and Mahrt, 1987). Then this model has been extended with a canopy resistance formulation and a surface run-off scheme by Chen *et al.* (1996) and implemented into the MM5 and WRF model for the model coupling system. In the Noah LSM of the coupled model, ET is expressed as the sum of direct evaporation from ground and canopy surface and transpiration through vegetation (Chen and Dudhia, 2001). Direct ground evaporation (EDIR) is estimated from a simple linear method (Betts *et al.*, 1997) and canopy surface evaporation (EC) is calculated from similar methods of Noilhan and Planton (1989) and Jacquemin and Noilhan (1990). Vegetation transpiration (ETT) is very similar to the EC formulation, but canopy resistance is included in its calculation. The canopy resistance which has been extended by Chen *et al.* (1996) in the Noah LSM is estimated by the formulation of Jacquemin and Noilhan (1990), representing the effects of solar

radiation, vapor pressure deficit, air temperature and soil moisture. The main procedure of the estimation process of surface moisture flux in Noah LSM is as follows. Once obtaining initial land states, surface characteristics and atmospheric forcing data, the model calculates land-atmospheric heat and moisture exchange coefficients with soil conductivity and diffusivity. Then, these coefficients are used to estimate potential evaporation which becomes the basis of the moisture flux estimation after combined with the canopy resistance.

The coupled WRF/Noah model has two major problems which are: (1) overestimation of latent heat flux (LH) probably induced by vegetation effects and (2) absence of routine soil moisture observations at regional and global scale for the model initial condition. In the previous study (Hong *et al.*, 2008), even though proper soil moisture initialization from field observation data for several locations resulted in reasonable simulations of soil moisture variations, LH simulations responded very sensitively to those variations, showing overestimations when soil moisture and vegetation amount were relatively high. In the Noah LSM, vegetation fraction (Fg), which is defined as area ratio of vegetation and defined area such as a pixel, plays a very important role in the determination of the each component of ET. However, Fg parameter, used in the current LSM, came from 5-yr monthly Advanced Very High Resolution Radiometer (AVHRR) data (1986–1991) with 0.15° spatial resolution which is about 15 km in Central America (Gutman and Ignatov, 1998). Considering that one of the merits of the recently advanced WRF model is to provide simulations with very high resolution of 1 km or even higher, the Fg parameter in the coarser resolution may effect negatively on the model accuracy and reliability for finer scale simulations. In terms of temporal resolution, monthly Fg data cannot provide enough information to describe short term variations of land cover such as in weekly or bi-weekly periods (Hong *et al.*, 2007). Anthropogenic activities such as crop harvest may cause a big change of land cover in just a few weeks. Moreover, interannually invariant Fg parameter is not congruous to annual land cover changes. Thus, Fg is required to be parameterized with more compatible temporal and spatial resolution for improved model simulations.

Absence of routine soil moisture measurement data at regional and global scale is obviously followed by low reliability of the model simulations. There are currently available input sources for usage of the model initialization such as National Center for Environmental Prediction (NCEP) final analysis data with 1 degree and 6 hour resolution, NCEP/NCAR Reanalysis data with 2.5 degree and 6 hour resolution, NCEP GRIB Global Data Assimilation System (GDAS) with 2.5 degree and 12 hour resolution and NCEP regional operational Eta with 40 km and 6 hour resolution. When the coupled MM5/Noah model was designed by Chen and Dudhia (2001), the Eta model simulation data were selected for the model initialization due to their relatively high spatial resolution for initial land states, large spatial coverage over North American area and similar physics of atmospheric forcing as used in Noah LSM. For the same reason of the Fg parameter above, 40 km resolution of Eta model is not compatible to finer model simulations, for example, with 1 km resolution which is used in this study. Coarse resolutions of initial data are generally followed by more interpolations to produce finer resolution outputs in the model. The differences in these spatial resolution causes model biases.

Ground Observation Data and Model Configuration Over the IHOP_2002 Area

The main goal of IHOP_2002 is to obtain accurate and reliable measurements of near surface moisture status which is very important for meteorological parameterization 2002 (Weckwerth *et al.*, 2004). These observations were carried out during a growing season from May to June 2002 with various field facilities. During the IHOP_2002 period, NCAR and University of Colorado installed surface flux stations, called Integrated Surface Flux Facilities (ISFF), to support the IHOP_2002 atmospheric boundary mission in Southern Great Plains (Chen *et al.*, 2003). The 9 ISFFs installed by NCAR, which were located in between Eastern Kansas and the Oklahoma Panhandle, are categorized as western (sites 1, 2 and 3), central (sites 4, 5 and 6) and eastern (sites 7, 8 and 9) tracks (Figure 2). The stations along the western track are located in south to north of the Oklahoma panhandle and the ones along the central and eastern track are aligned west to east in southwest of Wichita, Kansas. The area around the each station track shows characteristic surface condition related to soil moisture and vegetation cover. Along the western track, MODIS NDVI was in between 0.1 ~ 0.4 and soil moisture at 5 cm depth was less than 0.1 m^3m^{-3} in a dry period from 20 May to 27 May 2002. On the other hand, the eastern area including the eastern ISFF stations showed relatively high soil moisture with over 0.3 m^3m^{-3} in

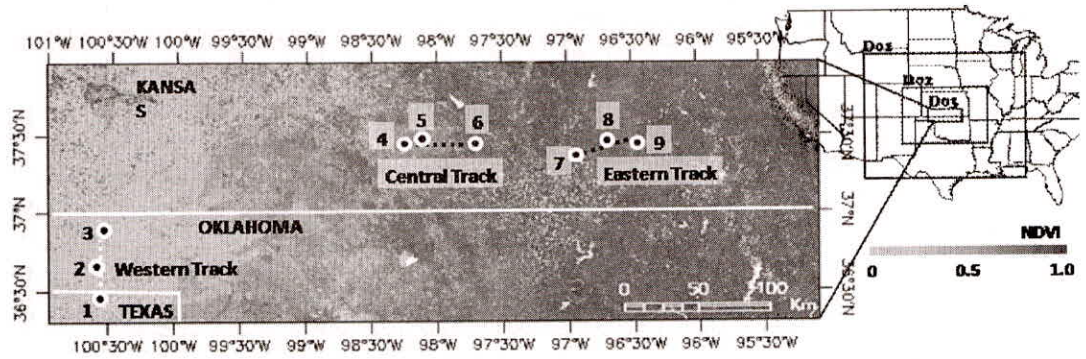

Fig. 2: Image of the study area with MODIS NDVI distribution over the IHOP_2002 study region and the model domain configuration scheme; dots with denoted numbers in the image indicate the locations of the 9 ISFF stations

average and high NDVIs in between 0.5 ~ 0.9. To sum up, the eastern area has more vegetation and cooler surface than does the western area (LeMone *et al.*, 2007).

The domain configuration was set up to cover all NCAR ISFF stations with 1 km resolution (Figure 2). We set three nesting domains with 5:1 spatial ratio. From the set of the subject domain (Domain 3) over IHOP_2002 area with 1 km resolution, an outer domain (Domain 2) was set with 5 km and then the mother domain (Domain 1) was set to cover about half of North America with 25 km resolution. Such domain configuration is controlled by domain nesting system which allows us to increase the model spatial resolution by the mesh refinement method (Michalakes, 2000). Through this domain nest setting, smaller domains with higher resolutions take and/or give information about boundary conditions from bigger domains with lower resolutions. The covering area of each domain comprises 75 by 55, 206 by 106 and 526 by 186 grid boxes for the domain 1, 2 and 3, respectively and each grid box represents a square area with the given length from the resolutions (25 by 25, 5 by 5 and 1 by 1 km, respectively).

Based on the soil moisture time series obtained from the field measurements, we set three simulating time configurations which are expected to represent the temporal heterogeneity of surface moisture status. According to the ISFF observations, each station showed relatively dry period until a rainfall event on between 24 and 27 May 2002 and then the relatively high surface moisture condition gradually decreased until the next rainfall event around 4 June 2002. We set the high moisture period of the surface on between 24 and 27 May as WET period and then the dry period before the WET as DRY1 and the one after the WET as DRY2. With this setting, we expected the sensitivity of the model response to the variation of the surface moisture condition when it goes from dry to wet period or *vice versa*. We set the model spin-up time for each period with 48 hours: from 22 May 00:00 to 24 May 00:00 for DRY1, from 28 May 00:00 to 30 May 00:00 for WET and from 2 June 12:00 to 4 June 12:00 for DRY2.

Model Parameterization and Initialization

We tested the model sensitivities to changes of vegetation parameter and soil moisture initial condition through vegetation fraction (Fg) parameterization and soil moisture initialization. There are two popular methods for deriving Fg. One is used in the current coupled WRF/Noah model and derived by the following linear method (Gutman and Ignatov, 1998),

$$Fg = \frac{NDVI - NDVI_{min}}{NDVI_{max} - NDVI_{min}} \quad \ldots (1)$$

where $NDVI_{min}$ is minimum NDVI (or bare soil NDVI) and $NDVI_{max}$ is maximum NDVI (or full canopy NDVI). The current model uses 0.04 for $NDVI_{min}$ and 0.54 for $NDVI_{max}$ which have been selected as seasonally and geographically invariant constants (Gutman and Ignatov, 1998) and the monthly Fg data using global 5-year AVHRR NDVI (1986 to 1991) have been applied to the model Fg parameter. The other popular method to compute Fg is the quadric model (Carlson and Ripley, 1997),

$$Fg = \left(\frac{NDVI - NDVI_{min}}{NDVI_{max} - NDVI_{min}} \right)^2 \quad \ldots (2)$$

Montandon and Small (2008) pointed out that underestimation of $NDVI_{min}$ causes overestimation of Fg specially in sparse vegetation area such as grassland in the western area and this overestimation is minimized when using the quadric Fg method.

Considering the relatively high spatial and temporal resolution for new Fg parameters, we produced Fg

from the MODIS data as mentioned above. There are two different MODIS platforms: Terra and Aqua, but we only used data from Terra MODIS due to data availability in 2002. To derive NDVI, we obtained 8-day 500 m surface reflectance from MODIS via http://lpdaac.usgs.gov and NDVI is calculated as follows,

$$\mathrm{NDVI} = \frac{\mathrm{NIR} - R}{\mathrm{NIR} + \mathrm{R}} \quad \ldots (3)$$

where R is red infrared reflectance and NIR is near infrared reflectance. Those reflectances correspond to the MODIS sensor band 1 (620–670 nm) and band 2 (841–876 nm), respectively. Even though MODIS provides daily surface reflectance which may be able to offer vegetation variation in daily basis, the data are not usable for this study due to data loss caused by cloud effects. Most recent studies have used 16 day MODIS NDVI imagery for deriving Fg (e.g., Miller *et al.*, 2006; Montandon and Small, 2008), but we selected 8-day MODIS reflectance to approach as closely to the temporal resolution configured in this study. The MODIS data sets were spatially resized from 500 m to 1 km, 5 km and 25 km resolutions through data aggregation for domain 1, 2 and 3, respectively. Then, based on the quality information of the MODIS data, bad data pixels, contaminated by cloud effects, were eliminated and replaced to a null value. The applied MODIS data sets to the Fg parameterizations are 8-day 17 May 2002 data granules for DRY1 and 8-day 25 May 2002 data granules for WET and DRY2.

For the determination of $\mathrm{NDVI}_{\mathrm{min}}$ and $\mathrm{NDVI}_{\mathrm{max}}$, we used two different methods. One is to select them as invariant constant values among the local MODIS NDVIs in our study area (domain 3). In our case, the selected NDVI values were 0.04 and 0.80 for $\mathrm{NDVI}_{\mathrm{min}}$ and $\mathrm{NDVI}_{\mathrm{max}}$, respectively. The other method used in this study is to use a constant $\mathrm{NDVI}_{\mathrm{min}}$ but variant $\mathrm{NDVI}_{\mathrm{max}}$. In the physics of canopy resistance applied to the Noah LSM, vegetation parameters such as maximum/minimum stomatal resistance, leaf area index and leaf cuticular resistance have constant values for each land cover type. Thus, it is likely to be more beneficial to obtain better LH simulation, if Fg derivation is associated with land cover types. In this study, we adopted a constant $\mathrm{NDVI}_{\mathrm{min}}$ (0.07) and variant $\mathrm{NDVI}_{\mathrm{max}}$ which were derived using Zeng *et al.* (2000) method for 2003 MODIS NDVI data as in the study of Montandon and Small (2008). Table 1 summarizes the methods used for the Fg parameterizations in this study. We named each method as BASE, VEG1 and VEG2 as shown in Table 1.

In order to provide improved land-state initialization for the coupled WRF/Noah model, HRLDAS is being developed at NCAR and executed in uncoupled mode of the Noah LSM by interpolating land surface variables from observed atmospheric forcing conditions (Chen *et al.*, 2007). An advantage of HRLDAS is the consistency with the coupled WRF/Noah model system because it uses the same WRF nested grid configuration such as resolution, grid points and projection and the same land surface parameters such as land use, soil texture, terrain height and vegetation properties. HRLDAS reads those sources from WRF input files generated by WRF Standard Initialization (SI) or WRF Preprocessing System (WPS). Atmospheric forcing data used on HRLDAS includes hourly 4 km NCEP stage-IV rainfall analyses data (Fulton *et al.*, 1998), hourly 0.5-degree downward solar radiation derived from the Geostationary Operational Environmental Satellite (GOES) (Pinker *et al.*, 2003) and three-hourly atmospheric analyses from NCEP Eta Data Assimilation System (EDAS) (Rogers *et al.*, 1995). With the model basis of Noah LSM, HRLDAS uses four soil layers to present daily, weekly and seasonal soil moisture variation.

In this study, we produced input files for HRLDAS using WRF SI. Chen *et al.* (2007) experimented HRLDAS spin-up dependency to find out its equilibrium state for various soil layers and pointed out that fine soil texture with low hydraulic conductivity requires longer spin-up time to reach the equilibrium state. Based on their study we ran HRLDAS for about 13 months which is a typical runtime span for most soil types for their equilibrium, starting from April 2001. The soil moisture generated by HRLDAS was used for the model initial conditions, combined with the quadric Fg model parameterization method.

Table 1: Summary of the Coupled Model Simulations

CASE	*BASE*	*VEG1*	*VEG2*	*HRLDAS*
Fg Parameter	Monthly AVHRR Linear	8 day MODIS Linear	8 day MODIS Quadric	8 day MODIS Quadric
Soil Moisture Initial condition	40 km NCEP Eta	40 km NCEP Eta	40 km NCEP Eta	1 km HRLDAS

RESULT

Satellite Data Comparisons

We investigated how surface temperature varies with NDVI and VegWC. Figure 3 shows (a) General description about the relationship between Ts and NDVI (or vegetation greenness) and (b) the relationship diagrams for the study regions. This relationship, termed as the TvX relationship, has been examined in many previous studies as a fundamental descriptor of the land surface state related with surface moisture availability and hence ET (Nemani and Running, 1989; Sandholt *et al.*, 2002). The geometry of the TvX relationship shows regional, climatic and biome dependence (Goetz, 1997; Sandholt *et al.*, 2002) and our study regions fall within the triangle-shaped geometry, showing a good contrast of general climatic and vegetation characteristics in each study region. The clustering of the points from each of the three regions on the TvX plot shows the importance of climate and vegetation characteristics. The TvX relationship of the NAMS region in the figure is distributed in the range of upper and left area, which indicates very low vegetation and dry condition with high potential evaporation. The IHOP region in this relationship shows relatively wetter climate than the NAMS region with more partial canopy. Tifton, GA, on the other hand, shows fully vegetation and very wet climate with high potential transpiration. With low evaporation, Ts of bare soil is much higher than that of plant canopies and therefore a negative slope exists along the dry or warm edge. This slope in the TvX relationship is steeper in dryer conditions (Goetz, 1997; Nemani *et al.*, 1993). In Figure 4, the steepness of the negative slopes is higher in the NAMS region. Through the regression analyses of the TvX relationship, the statistical correlation in the NAMS region is much stronger, compared with Tifton, GA. NVegWC has been color-coded into this TvX relationship in Figure 4, showing high NVegWC distributed in higher Ts and lower NDVI areas.

Figure 5 shows the NVegWC variation range for each land cover type. Even in the same vegetation type, NVegWC variations are different in each region and the average values in the NAMS region are generally higher with wider variation range while Tifton, GA shows much less variation of NVegWC with lower average values than the other regions. The major types of vegetation in the NAMS region (shrublands and savannas) show relatively high NVegWC with very high variation. Thus, the result in Figure 3 can be explained as the tendency of vegetation behavior, which is high water-leaf vegetation with low NDVI indicating more water exists in vegetation leaves of more arid environments. Arid regions with low NDVI, however, do not have a continuous canopy cover but a sparse coverage, for example, clumps of vegetation interspersed with bare soil area. Since Ts of bare soils is always lager, for daytime measurements, than that of transpiring vegetation in summer season, Ts of the NAMS region is higher than that of the other two regions, considered in this study (the Figure 3 and 4). Because of this influence of discontinuous vegetation coverage on Ts, the relationship between NVegWC and Ts in such arid areas can be overstated, but the NVegWC - NDVI relation provides enough clues for the conclusions reached in this study.

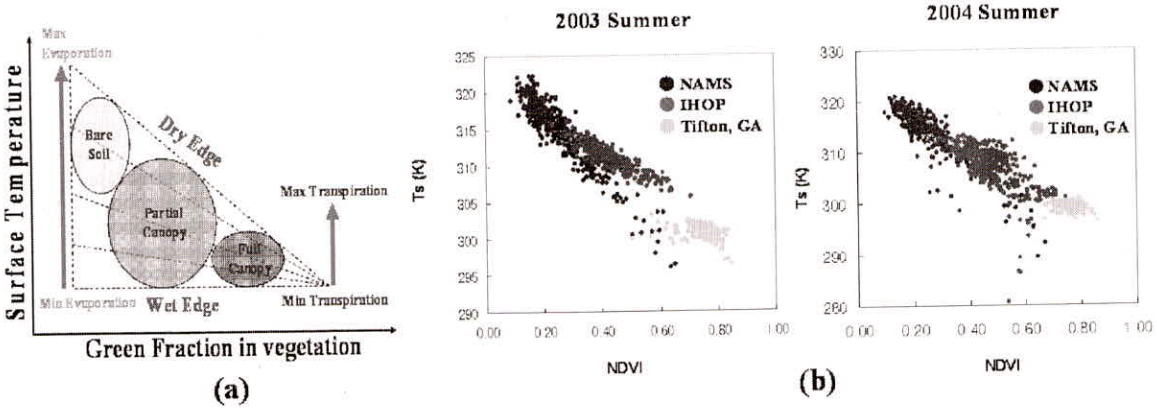

Fig. 3: (a) A schematic TvX relationship and (b) regional TvX distributions of three regions

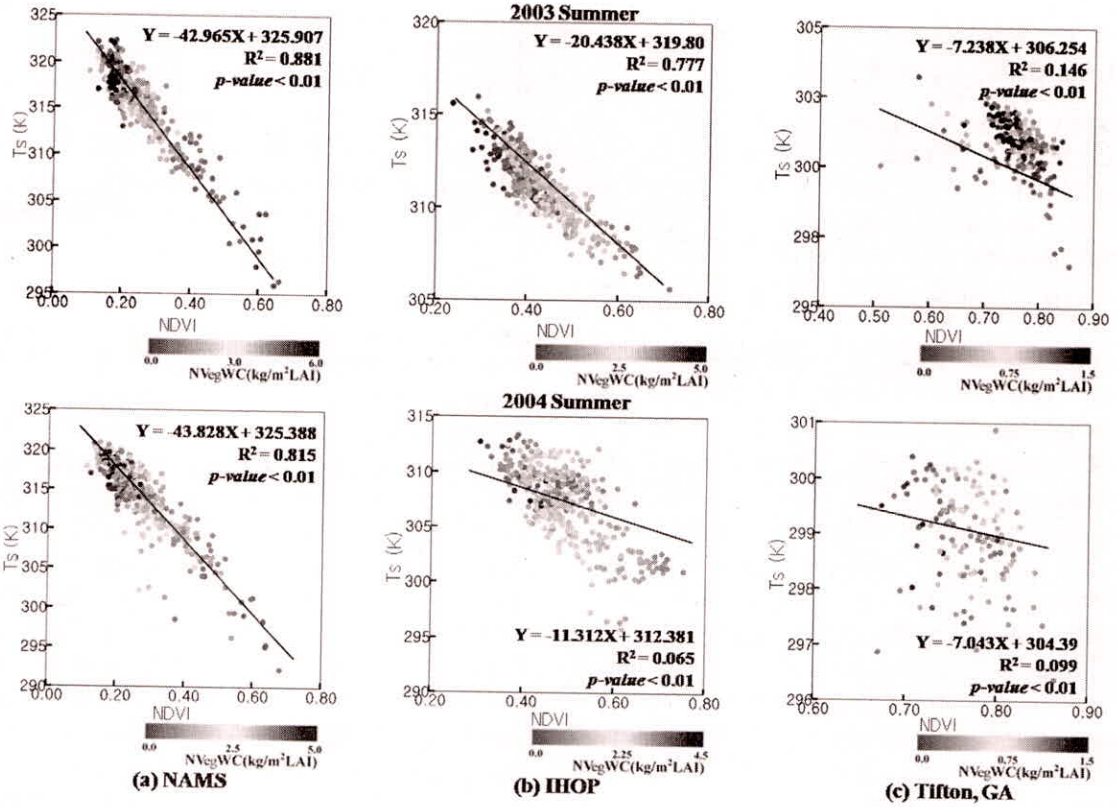

Fig. 4: The regression analysis of the TvX relationships color-coded with NVegWC: (a) the NAMS region, (b) the IHOP region and (c) Tifton, GA

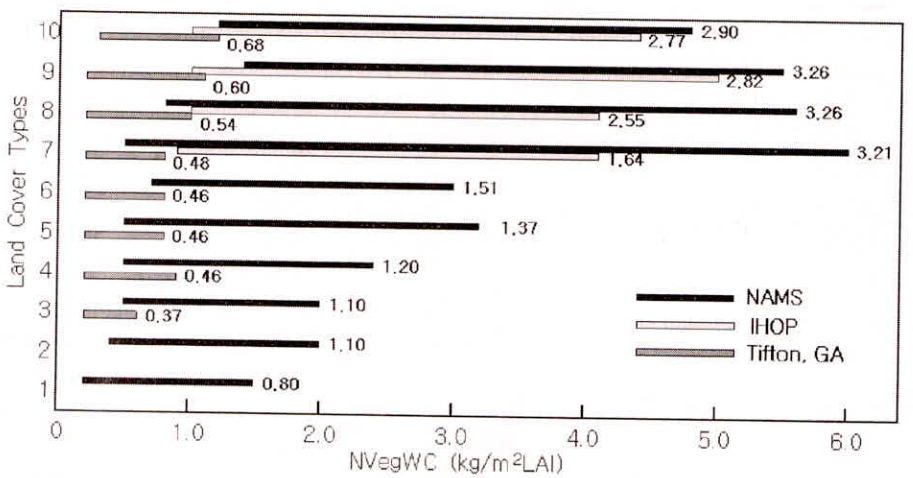

Fig. 5: NVegWC variation in different land cover types for summer season of 2003 and 2004 (the numbers of land cover types follow the IGBP classification). The denoted numbers are the NVegWC average values for each range bar

Coupled Model Tests

Figure 6 shows the temporal variations of simulated land surface variables and Table 2 provides their statistical comparisons to the ISFF observations with correlation coefficients (R-square values from regression analyses) and Root Mean Square Errors (RMSE). Relatively low correlations were observed in GH and LH in the eastern area while the other areas showed good correlations with the observations. The comparisons of their temporal variations and RMSE make possible various interpretations.

In order to test only vegetation effect by Fg parameterization, soil moisture initial values for the 9 ISFF station sites were replaced by the observed data. With this data replacement for the soil moisture initial condition, low atmospheric variation in each simulation

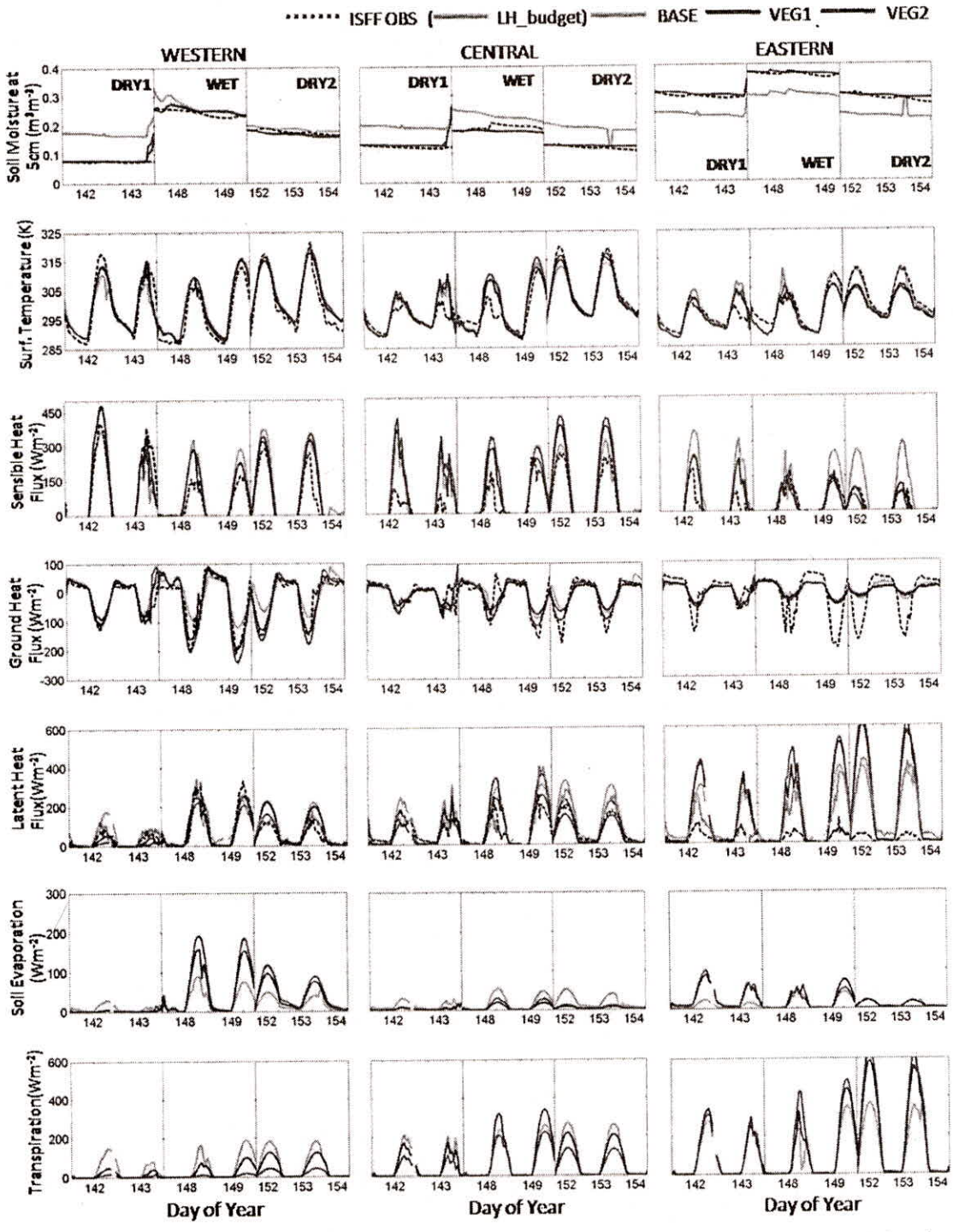

Fig. 6: Temporal variations of land surface variables simulated by the WRF/Noah model and their comparisons to the ISFF observations for the BASE, VEG1 and VEG2 cases

period resulted reasonable soil moisture simulations in the coupled WRF/Noah model; there was no observation of any substantial rainfall during each period, except from 5 to 20 mm of precipitation at the end of DRY1. Generally the soil moisture initial conditions were adjusted to be lowered in the western and central areas and to be raised in the eastern area.

The effects of Fg parameter on surface temperature (TS) simulation were observed mainly during DRY2 in the eastern area, showing about 5 K decrease of the diurnal peaks, while those of the other regions showed slight or no improvement. RMSE of TS simulations, however, did not show any significant difference among the cases. The average RMSE of TS simulations were

Table 2: Correlation Coefficients and Root Mean Square Errors (RMSE) of Simulated Land Surface Variables to ISFF Observations

		Western		Central		Eastern	
		R^2	RMSE	R^2	RMSE	R^2	RMSE
TS (K)	BASE	0.86	3.71	0.78	3.57	0.82	2.91
	VEG1	0.92	3.09	0.81	3.41	0.82	2.98
	VEG2	0.91	3.47	0.79	3.95	0.78	3.30
	HRLDAS	0.92	3.83	0.80	4.01	0.79	2.90
SH (Wm^{-2})	BASE	0.67	78.28	0.68	76.35	0.62	91.07
	VEG1	0.81	62.60	0.75	85.90	0.73	38.33
	VEG2	0.78	70.16	0.73	106.55	0.69	40.74
	HRLDAS	0.86	68.53	0.80	102.86	0.67	63.85
GH (Wm^{-2})	BASE	0.80	36.56	0.60	33.37	0.66	51.25
	VEG1	0.89	24.23	0.72	30.02	0.62	52.03
	VEG2	0.89	33.53	0.74	27.38	0.50	54.09
	HRLDAS	0.89	42.72	0.73	28.39	0.50	54.47
LH (Wm^{-2})	BASE	0.72	47.51	0.81	69.57	0.58	151.52
	VEG1	0.76	39.66	0.80	58.57	0.56	218.63
	VEG2	0.83	33.14	0.75	37.03	0.53	234.86
	HRLDAS	0.94	39.64	0.77	34.99	0.49	188.61
LH_ Budget (Wm^{-2})	BASE	0.74	46.70	0.73	63.67	0.81	61.94
	VEG1	0.79	40.72	0.70	59.03	0.87	100.80
	VEG2	0.83	38.05	0.66	57.92	0.87	114.43
	HRLDAS	0.90	44.91	0.70	60.53	0.91	69.46

about 3 K. The TS underestimation in the eastern area is the locations where soil moisture was around 0.38 m^3m^{-3}, but this does not indicate soil moisture effect from the data replacement but rather the vegetation effect from the Fg parameterizations. Increase in Fg amount caused lowered the TS. This is also supported by the HRLDAS test as described in the next section.

While TS underestimations were observed, Sensible Heat (SH) simulations showed significant improvement during especially WET and DRY2 in the eastern area. The SH simulations agree very closely with the observations with about 200 Wm^{-2} decrease during DRY2 in that region. RMSE of SH also supports this improvement which was observed in both of the Fg parameterizations. In the eastern area, RMSE of SH improved from 91.07 Wm^{-2} to about 40 Wm^{-2}. SH values of the diurnal peaks in that region decreased by 100 Wm^{-2} during DRY1, 120 Wm^{-2} during WET and 200 Wm^{-2} during DRY2 which are very close values to the SH observations. No substantial difference between VEG1 and VEG2 was observed because Fg parameters were very similar in the eastern stations. On the other hand, SH during DRY2 in the central track showed overestimations and increased by 100 Wm^{-2} from that of the BASE case. RMSEs also increased by 30 Wm^{-2} in the VEG2 case. The other periods (DRY1 and WET) in the central area showed no significant changes in SH simulations. Meanwhile, in the western area, less influence of Fg parameter was observed and SH overestimation during DRY1 of the VEG1 and VEG2 cases is interpreted as the model high sensitivity to soil moisture variation in that region.

Ground heat flux (GH) simulations did not show any vegetation effect in the high vegetated areas, showing low correlations and hence low reliability in the GH simulations of the model. The low diurnal variations of simulated GH in the eastern area were not improved either by the Fg parameterizations or soil moisture initialization. GH RMSEs in this region showed over 50 Wm^{-2} which is more about 20 Wm^{-2} than those of the other regions. Considered that the range of the GH diurnal cycle (from about 80 Wm^{-2} to 200 Wm^{-2}), this error is quite significant. The greatest difference between the observations and the simulations were up to 150 Wm^{-2}. On the other hand, some simulation improvements especially in the VEG1 case were observed during WET and DRY2 in the low vegetated region (the western area).

Latent Heat (LH) simulations were very sensitive to Fg in highly vegetated area. The stations in the eastern track were contaminated, so we used the radiation budget method for the LH calculation with measured net radiation (R), SH and GH in this study, naming it "LH_budget". The correlations of LH simulations with the observations have been substantially improved when it was compared with LH_Budget data set. Noticeable LH overestimations in that area were observed and the differences from the LH_budget observation were as much as 200 Wm^{-2}. This LH overestimation has been also reported in previous studies (Chen *et al.*, 2007; Hong *et al.*, 2008) in both of which used the same Noah LSM implemented into HRLDAS and into the WRF model, respectively. Any substantial difference between the VEG1 and VEG2 cases was not observed in the eastern region, but the central (in all periods) and western areas (during DRY2) show improved simulations in the VEG2 case. The error statistics through RMSEs of LH also demonstrates this phenomenon; RMSE were observed to be better in VEG1 (about 6 Wm^{-2} and 3.5 Wm^{-2} improvements in the western and central area, respectively) and VEG2 (about 7.5 Wm^{-2} and 6 Wm^{-2} improvements in the western and central area, respectively) cases in relatively low vegetated area but worse in the eastern area (about 39 Wm^{-2} and 52 Wm^{-2} worseness in VEG1 and VEG2 cases, respectively) as verified with LH_budget observations. When compared with LH observations, the central area shows better results with a lower RMSE (about 39 Wm^{-2} improvements in the VEG2 case). The analyses of the temporal variations of the ET components, EDIR and ETT, were performed in order to understand the LH overestimations in the eastern area. EC generally occurs in a very short time, taking very small portion of the total ET after precipitation. Since the model was configured to avoid any precipitation for clear sky conditions during the spin-up periods, we omitted analyzing EC in this result section. EC was very small portion in our model simulations (less than 10 Wm^{-2} in average) and can be ignored for LH analyses. According to the result, the LH overestimation is mainly due to the overestimation of vegetation transpiration. LHs were overestimated in both VEG1 and VEG2 cases with about 250 Wm^{-2} more than those of the BASE case. Hong *et al.* (2008) have more emphasized the soil moisture effect for these LH overestimations, but our study provides a different point of view. With the HRLDAS case study, we present that the vegetation effect is more responsible for the LH overestimation than soil moisture variation.

Figure 7 shows the temporal variation of the surface variables simulated by the coupled WRF/Noah model and Table 2 also provides the statistical analyses for this HRLDAS case. Briefly, relatively good correlations with observations were observed in most variables except GH and LH in the eastern area similarly as in Fg cases; R^2 was 0.5 for GH. The low coefficient of LH simulations was improved when it was compared to LH_budget (from 0.49 to 0.91). Soil moistures simulated by HRLDAS were improved in the western and central regions but showed almost no change in the eastern area. This soil moisture improvement, however, did not have significant effect on TS simulations, but the vegetation does have an impact and displays a very similar pattern of the TS diurnal cycle as that in VEG2 cases. Moreover, the TS underestimations in the eastern area support the Fg effect as discussed in the previous section. Meanwhile, the second TS peak values in the western area give us an interesting implication about the model. In the soil moisture variations of the VEG2 and HRLDAS cases, HRLDAS showed higher soil moisture (0.13 m^3m^{-3}) than that in VEG2 (0.08 m^3m^{-3}), but the second TS peak value during DRY1 was higher in HRDAS (319 K) than that in VEG2 (315 K). This result of the TS increase in spite of soil moisture increase in low vegetated area indicates a greater sensitivity of the model to Fg parameter but not to soil moisture even in such region (Fg was 0.09 in the western station sites of VEG2 in average).

Unlike the improved SH simulations in the VEG1 and VEG2 cases in the eastern track, the ones of HRLDAS did not resemble the observed diurnal cycle due to negligible soil moisture change in the region. This indicates that the SH simulation is affected not only by vegetation but also by soil moisture variation. While the central area showed similar results as in the VEG2 case, the western area indicated the model sensitivity to soil moisture variation as discussed in the previous section. During the WET period in the western area, soil moisture did not display any quantifiable variability in all cases in this study. This resulted in little change of SH simulations in that period, indicating low sensitivity to Fg parameter. On the other hand, while soil moisture was lowered to 0.1 m^3m^{-3} during DRY1 in that region, SH of the VEG2 case increased by about 100 Wm^{-2} in the first peak time of that period. A similar result was observed in the HRLDAS case (SH increased by 50 Wm^{-2}), but the difference in the SH peak values between these two cases explains the SH overestimation to be caused by soil moisture variation in such low vegetated area.

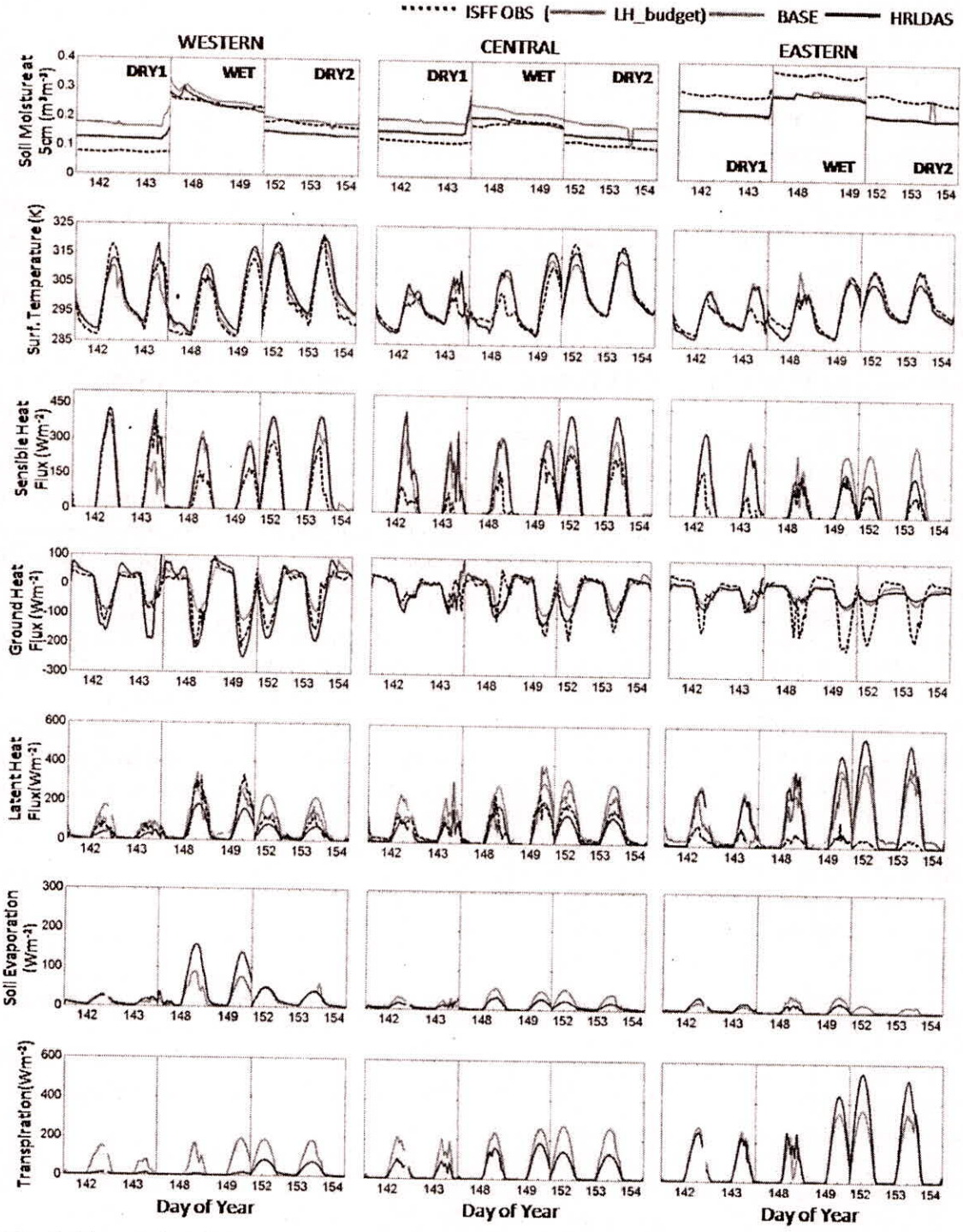

Fig. 7: Temporal variations of land surface variables simulated by the WRF/Noah model and their comparisons to the ISFF observations for the BASE and HRLDAS+VEG2 cases

GH in the coupled model is not sensitive to soil moisture variation, showing very similar results as the VEG1 and VEG2 cases, except relatively high fluctuations during DRY1 in the western area. This anomaly is assumed to be due to relatively high Ts simulation of the coupled model because GH estimation in the model physics is closely related to soil temperature which is regarded as TS in very low vegetated regions.

LH overestimations by ETT overestimation were also observed in the eastern area in the HRLDAS case, indicating vegetation effect. From the HRLDAS case study, however, we found that the soil moisture variation was also effective in the ETT overestimation.

Due to no soil moisture change in the HRLDAS case, ETT showed less overestimation (up to 550 Wm^{-2}) than that in the VEG1 or VEG2 case (up to 630 Wm^{-2}). Thus, the ETT difference between the HRLDAS and VEG1 or VEG2 cases implies effect of soil moisture variation. In the western area, the both effects of vegetation and soil moisture on ETT simulations were also observed; when Fg and soil moisture decreased during DRY1, ETT also decreased. EDIR simulations also support the dual effects; during WET in the western area, EDIR increased more up to about 200 Wm^{-2} by only Fg decrease than that by Fg and soil moisture decrease (up to about 160 Wm^{-2}). The RMSE of the LH simulations in the HRLDAS case showed significant improvement in the central area more than other cases (from comparisons with the LH observations). Meanwhile, they seem to show better result in the eastern area than that of the VEG1 or VEG2 case (from the statistics with the LH_budget), but this did not lead to any improvement from the BASE case (Table 2).

CONCLUSION

For the satellite variable comparisons, we have performed analyses of four land surface variables (VegWC, NDVI, LAI and Ts) to investigate their interactions, using satellite derived AMSR-E and MODIS data. Spatial variation of the relationship between them has been mainly focused through selecting three climatic characteristic regions in North America: the NAMS region, the IHOP region and Tifton, GA. Each region shows typical trends of arid or semi-arid and humid areas. During these analyses, we introduced a new variable, NVegWC and obtained remarkable results. The negative relationship between NVegWC and NDVI and between Ts and NDVI shows more water existence in plant leaves in more arid area and the determination coefficients for those relationships of each region in the regression analyses explain the dependency of vegetation on water condition. It is generally assumed that the greenness of vegetation is related to the photosynthesis and the photosynthesis is dependent on solar radiation and the amount of carbon dioxide. Water content in vegetation is also utilized for the photosynthesis by which oxygen is released into the atmosphere, causing plant transpiration. Water amount in vegetation is closely related to different vegetation types than the greenness of vegetation which is considered as an indicator of photosynthesis. The photosynthesis process in vegetation is controlled under water stress condition. There are many physiological and climate factors influencing vegetation water stress such as soil moisture and precipitation and that the surface temperature is one of the indicators of increased water stress. During the summer months, an increase in Ts implies an increase in water stress of vegetation, all other factors being equal and moreover in arid regions Ts is more likely to impact water stress of vegetation than other factors. Vegetation physiologically responds to high water stress condition by closing the stomata to control losing moisture and by having a deep and widely-spread root system to reach water sources in deeper soil (Tanguiling *et al.*, 1987; Cohen *et al.*, 2005). There are also some species, especially in arid area, that store more water in leaves during rainy season (Kramer, 1983). Weighing actual amount of water in different plant types separately for leaves, stems and fruits/flowers, Sims and Gamon (2003) showed that in drought deciduous shrubs contain more water in their leaves than that in evergreen tree leaves. These physiological responses of vegetation have been considered as adaptation mechanism to environment (Kramer, 1983) and they would be present more in vegetation in arid regions where the water stress is a normal situation. Hence, the dominant vegetation in arid area like the NAMS region is more likely to be adapted to their environment in a way to minimize their water loss than that in more humid area like Tifton, GA. In this study, LAI shows significant regional difference in values (NAMS : 0~2, IHOP : 0.5~2.5, Tifton, GA : 1.5~6), but the regional differences of VegWC values between the three regions is not as much (NAMS : 0~3 kg/m^2, IHOP : 1~4 kg/m^2, Tifton, GA : 1~4 kg/m^2). This can be explained as vegetation amount varies significantly under the regional climate condition, but the vegetation response shows a tendency to conserve water.

Through the model tests, the model sensitivity to vegetation and soil moisture variation was used to evaluate the model improvement from Fg parameterization and HRLDAS soil moisture initialization. The two Fg parameterization methods, the linear and quadric methods (VEG1 and VEG2, respectively), were used and they resulted the better spatial west-east contrast of Fg distribution: less vegetation in west and higher vegetation in east. In many cases of this study, vegetation effects on the coupled model simulations by the Fg parameterization were observed either positively or negatively in terms of the model improvement. We obtained underestimation of TS, overestimation of LH and improvements of SH in highly vegetated region (the eastern area) and underestimation of GH in low vegetated region (the

western area). According to the statistical analyses, we obtained improved results in SH simulations in the eastern area and in LH simulations in the western and central area for both VEG1 and VEG2 cases. Meanwhile, the HRLDAS case, combined with the VEG2 method, indicates both effects of vegetation and soil moisture variation. There was somewhat improvement from HRLDAS soil moisture initialization, but this needs to be validated through further research with a longer period of simulation.

Among the various changes after the Fg parameterizations and/or HRLDAS soil moisture initialization, noticeable results were found as the low GH variability and LH overestimation in the eastern stations. According to the physics in the Noah LSM, soil temperature plays a key role in GH estimations and soil temperature is function of soil moisture (Chen and Dudhia, 2001). Thus, in the VEG1 or VEG2 case of the western area, lowered GH peak values during WET and DRY2 are due to soil temperature increase induced by Fg decrease from the newer Fg parameterizations. In the same view, the fact that high Fg amount in the eastern area (over 0.7 in all study cases) resulted very low GH variability implies low soil temperature in that region possibly by canopy shadow effect. With both results, this study indicates high sensitivity of GH simulation to Fg parameter. Nonetheless, the low GH variability from the model in the eastern area is still problematic, compared to GH observations. This may imply excessive effect of vegetation.

On the other hand, LH simulations in the eastern area were also very sensitive to vegetation, showing overestimation of ETT. Finding the answer for the LH overestimation is quite challenging. The possible causes of LH overestimation of the model can be considered as follows: (1) initial soil moisture changes, (2) overestimation of wind velocity and (3) underestimation of air humidity at 2 m. The first case has been proved not to be much effective through this study. High wind intensity will be consequently followed by high ETT, but we could not observe any overestimation of wind from the model in the eastern area (Figure 8). Even though the wind velocity of the east-west component during DRY2 in that area somewhat increased after the Fg parameterizations, rather its lower variation from the model was observed compared to the wind observations (Figure 8). The last case cannot be also counted because the Noah LSM uses air humidity just as a diagnostic variable. The Noah LSM uses the lowest model-level humidity (Ek and Mahrt, 1991). Other possible answers about the ETT overestimations may be found in the relation with plant water stress and surrounding air condition such as CO_2 amount which affect the leaf stomata opening and closing which are the major factor to control vegetation transpiration (Betts *et al.*, 1997; Hong *et al*, 2007).

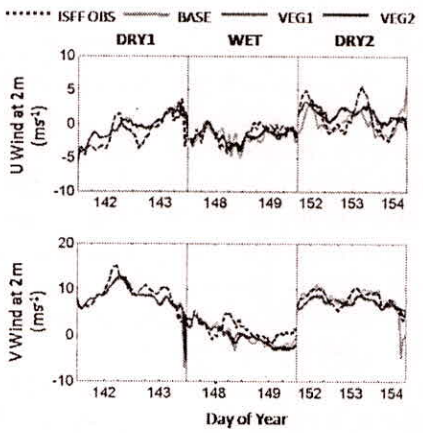

Fig. 8: Temporal variations of east-west (U) component (upper) and north-south (V) component (lower) wind velocity simulations and their comparison to the ISFF observations for the BASE, VEG1 and VEG2 cases in the eastern track

This study has shown the impact of vegetation on the complex land and atmospheric interactions through the analyses of remote sensing data and through the coupled model tests. In particular, the model sensitivity tests to the vegetation variation indicate the need of more practical quantification or understanding of vegetation properties for more improved model simulations. The model problem related to the sensitivity to vegetation fraction presents mainly in vegetation transpiration, showing its overestimations. Considered that proper parameterization of vegetation fractions did not significantly effect on the model improvement through this study, additional interpretations from new point of view about vegetation for the model physics may be more needed other than proper parameterization of vegetation properties. For example, the fact that the physiological responses of vegetation to surrounding environments vary with climatic conditions can provide an important hint to solve the model problem. In this study, the satellite-derived vegetation water content data played an important role to interpret the physiological responses. Although the vegetation water content data are still required to be validated, this variable can be further utilized to understand or quantify the vegetation behaviors. In addition, this study has shown that the importance of remote sensing data and their

demand are expected to increase in order to obtain more realistic land surface status for the model initial conditions such as soil moisture. Although limited observations of land surface processes are currently available from the remote sensing, continuous development of the satellite remote sensing technology will provide more practical information about the land-atmospheric interactions in the near future.

REFERENCES

Betts, R.A., Cox, P.M., Lee, S.E. and Woodward, F.I. (1997). "Contrasting physiological and structural vegetation feedbacks in climate change simulations". *Nature*, 387, 796–799.

Bosch, D.D., Davis, F.M. and Sheridan, J.M. (1999). "Rainfall characteristics and special correlation for the Georgia coastal plain". *Trans. ASAE*, 42(6), 1637–1644.

Carlson, T.N. and Ripley, D.A. (1997). "On the relation between NDVI, fractional vegetation cover and leaf area index". *Remote Sensing of Environment*, 62, 241–252.

Ceccato, P., Flasse, S. and Gregorie, J. (2002b). "Designing a spectral index to estimate vegetation water content from remote sensing data (part 2)". *Remote Sensing of Environment*, 82, 198–207.

Ceccato, P., Flasse, S., Tarantola, S., Jacquemoud, S. and Gregorie, J. (2001). "Detecting vegetation leaf water content using reflectance in the optical domain". *Remote Sensing of Environment*, 77, 22–33.

Chen, F., Mitchell, K., Schaake, J., Xue, Y., Pan, H., Koren, V., Duan, Q.Y., Ek, M. and Betts, A. (1996). "Modeling of land surface evaporation by four schemes and comparison with FIFE observations". *Journal of Geophysical Research*, 101(D3), 7251–7268.

Chen, F. and Dudhia, J. (2001). "Coupling an advanced land surface-hydrology model with the Penn State-NCAR MM5 modeling system. Part I: Model implementation and sensitivity". *Monthly Weather Review*, 129, 569–585.

Chen, F., Yates, D.N., Nagai, H., LeMone, M., Ikeda, K. and Grossman, R. (2003). "Land surface heterogeneity in the Cooperative Atmosphere Surface Exchange Study (CASES-97). Part I: Comparing modeled surface flux maps with surface-flux tower and aircraft measurements". *Journal of Hydrometeorology*, 4, 196–218.

Chen, F., Manning, K.W., LeMone, M.A., Trier, S.B., Alfieri, J.G., Roberts, R., Tewari, M., Niyogi, D., Horst, T.W., Oncley, S.P., Basara, J.B. and Blanken, P.D. (2007). "Description and evaluation of the characteristics of the NCAR High-Resolution Data Assimilation System". *Journal of Applied Meteorology and Climatology*, 46, 694–713.

Cohen, Y., Alchanatis, V., Meron, M., Saranga, Y. and Tsipris, J. (2005). "Estimation of leaf water potential by thermal imagery and spatial analysis". *J. Experimental Botany*, 56(417), 1843–1852.

Ek, M. and Mahrt, L. (1991). "OSU 1-D PBL model user's guide". Version 1.04, 120 pp. [Available from Department of Atmospheric Sciences, Oregon State University, Corvallis, OR 97331–2209.]

Fulton, R.A., Breidenbach, J.P., Seo, D.J.S., Miller, D.A. and O'Bannon, T. (1998). "The WSR-88D rainfall algorithm". *Weather and Forecasting*, 13, 377–395.

Goetz, S.J. (1997). "Multi-sensor analysis of NDVI, surface temperature and biophysical variables at a mixed grassland site". *Int. J. Remote Sensing*, 18(1), 71–94.

Gutman, G. and Ignatov, A. (1998). "The derivation of the green vegetation fraction from NOAA/AVHRR data for use in numerical weather prediction models". *International Journal of Remote Sensing*, 19(8), 1533-1543.

Hong, S., Lakshmi, V. and Small, E.E. (2007). "Relationship between vegetation biophysical properties and surface temperature using multi-sensor satellite data". *Journal of Climate*, 20, 5593–5606.

Hong, S., Lakshmi, V., Small, E.E. and Chen, F. (2008). "Interactions between the land surface and the atmosphere: Results from the Noah LSM and the WRF model". *Journal of Hydrometeorology., submitted.*

Jacquemin, B. and Noilhan, J. Noilhan (1990). "Sensitivity study and validation of a land surface parameterization using the HAPEX-MOBILHY data set". *Boundary-Layer Meteorology*, 52, 93–134.

Justice, C.O., Vermote, E., Townshend, J.R., Defries, R., Roy, D.P., Hall, D.K., Salomonson V.V., Privette, J.L., Riggs, G., Strahler, A., Lucht, W., Myneni, R.B., Knyazikhin, Y., Running, S.W., Nemani, R.R., Wan, Z., Huete, A.R., Leeuwen, W.V., Wolfe, R.E., Giglio, L., Muller, J.P., Lewis, P. and Barnsley, M.J. (1998). "The Moderate Resolution Imaging Spectroradiometer (MODIS): Land remote sensing for global change research". *IEEE Trans. Geoscience & Remote Sensing*, 36(4), 1228–1249.

Kleidon, A. and Heimann, M. (1998). "Optimized rooting depth and its impacts on the simulated climate of an atmospheric general circulation model". *Geophysical Research Letters*, 25(3), 345–348.

Kramer, P.J. (1983). "Water Relations of Plants". *Academic Press.*

Kurc, S. and Small, E.E. (2004). "Dynamics of evapo-transpiration in semi-arid grassland and shrubland during the summer monsoon season, central New Mexico". *Water Resources Research,* 40. 9, 10, 1029.

LeMone, M.A., Chen, F., Alfieri, J.G., Tewari, M., Geerts, B., Miao, Q., Grossman, R.L. and Coulter, R.L. (2007). "Influence of land cover and soil moisture on the horizontal distribution of sensible and latent heat flux in Southeast Kansas during IHOP_2002 and CASES-97". *Journal of Hydrometeorology*, 8, 68–87.

Mahrt, L. and Ek, K. (1984). "The influence of atmospheric stability on potential evaporation". *Journal of Applied Meteorology*, 23, 222–234.

Michalakes, J. (2000). "A parallel runtime system library for regional atmospheric models with nesting, in Structural

Adaptive Mesh Refinement (SAMR) grid methods". *IMA Volumes in Mathematics and Its Applications (117)*, Springer, New York, 59–74.

Miller, J., Barlage, M., Zen, X., Wei, H., Mitchell, K. and Tarpley, D. (2006). "Sensitivity of the NCEP/Noah land surface model to the MODIS green vegetation fraction data set". *Geophysical Research Letters*, 33, L130404, doi:10.1029/2006GL026636.

Montandon, L.M. and Small, E.E. (2008). "The impact of soil reflectance on the quantification of the green vegetation fraction from NDVI". *Remote Sensing of Environment*, 112, 1835–1845.

Myneni, R.B., Hall, F.G., Sellers, P.J. and Marshak, A.L. (1995). "The interpretation of spectral vegetation indexes". *IEEE Trans. Geoscience & Remote Sensing*, 33(2), 481–486.

Myneni, R.B., Ramakrishna, R., Nemani, R. and Running, S. (1997). "Estimation of global leaf area index and absorbed PAR using radiative transfer models". *IEEE Trans. Geosciece & Remote Sensing*, 35(6), 1380–1393.

Myneni, R.B., Hoffman, S., Knyazikhin, Y., Privette, J.L., Glassy, J., Tian, Y., Wang, Y., Song, X., Zhang, Y., Smith, G.R., Lotsch, A., Friedl, M., Morisette, J.T., Votava, P., Nemani, R.R. and Running, S.W. (2002). "Global products of vegetation leaf area and fraction absorbed PAR from year one of MODIS data". *Remote Sensing of Environment*, 83, 214–231.

Nemani, R., Pierce, L., Running, S. and Goward, S. (1993). "Developing satellite-derived estimates of surface moisture status". *J. Applied Meteorology*, 32, 548–557.

Nemani, R. and Running, S. (1989). "Estimation of regional surface resistance to evapotranspiration from NDVI and Thermal-IR AVHRR data". *J. Applied Meteorology*, 28, 276–284.

Noilhan, J. and Planton, S. (1989). "A simple parameterization of land surface processes for meteorological models". *Monthly Weather Review*, 117, 536–549.

Njoku, E.G. and Chan, T. (2005). "Vegetation and surface roughness effects on AMSR-E land observations". *Remote Sensing of Environment,* 100(2), 190–199.

Njoku, E.G., Jackson, T., Lakshmi, V., Chan, T. and Nghiem, S. (2003). "Soil moisture retrieval from AMSR-E". *IEEE Trans. Geoscience & Remote Sensing*, 41, 215–229.

Njoku, E.G. and Li, L. (1999). "Retrieval of land surface parameters using passive microwave measurements at 6–18 GHz". *IEEE Trans. Geoscience & Remote Sensing*, 37(1), 79–93.

Pan, H.L. and Mahrt, L. (1987). "Interaction between soil hydrology and boundary-layer development". *Boundary-Layer Meteorology*, 38, 185–202.

Pielke, R.A. (2001). "Influence of the spatial distribution of vegetation and soils on the prediction of cumulative rainfall". *Review of Geophysics*, 39(2), 151–177.

Pinker, R.T., Tarpley, J.D., Laszlo, I., Mitchell, K.E., Houser, P.R., Wood, E.F., Schaake, J.C., Robock, A., Lonmann, D., Cosgrove, B. A., Sheffiedl, J., Duan, Q., Luo, L. and Higgins, R.W. (2003). "Surface radiation budgets in support of the GEWEX Continental Scale International Project (GCIP) and the GEWEX Americas Prediction Project (GAPP), including the North American Land Data Assimilation System (LDAS) Project". *Journal of Geophysical Research*, 108, 8844, doi:10.1029/2002JD003301.

Rogers, E., Deaven, D.G. and DiMego, G.J. (1995). "The regional analysis system for the operational "early" Eta model: Original 80-km configuration and recent changes". *Weather and Forecasting*, 10, 810–825.

Sandholt, I., Rasmussen, K. and Andersen, J. (2002). "A simple interpretation of the surface temperature/vegetation index space for assessment of surface moisture status". *Remote Sensing of Environment*, 79, 213–224.

Shibata, A., Imaoka, K. and Koike, T. (2003). "AMSR/AMSR-E level 2 and 3 algorithm developments and data validation plans of NASDA". *IEEE Trans. Geoscience & Remote Sensing*, 41, 195–203.

Sims, D.A. and Gamon, J.A. (2003). "Estimation of vegetation water content and photosynthetic tissue area from spectral reflectance: a comparison of indices based on liquid water and chlorophyll absorption features". *Remote Sensing of Environment*, 84, 526–537.

Skamarock, W.C., Klemp, J.B., Dudhia, J., Gill, D.O., Barker, D.M., Wang, W. and Powers, J.D. (2005). "A description of the advanced research of WRF version 2". *Technical report, National Center for Atmospheric Research*, TN-468+STR.

Small, E.E. and Kurc, S. (2003). "Tight coupling between soil moisture and the surface radiation budget in semi-arid environments: Implications for land-atmosphere interactions". *Water Resources Research*, 39(10), 1278.

Tanguiling, V.C., Yambao, E.B., Toole, J.C.O. and De Datta, S.K. (1987). "Water stress on leaf elongation, leaf water potential, transpiration and nutrient uptake of rice, maize and soybean". *Plant and Soil*, 103, 155–168.

Tucker, C.J. (1979). "Red and photographic infrared linear combination for monitoring vegetation". *Remote Sensing of Environment*, 8, 127–150.

Wan, Z. and Li, Z.L. (1997). "A physics-based algorithm for retieving land-surface emissivity and temperature from EOS/MODIS data". *IEEE Trans. Geoscience & Remote Sensing*, 35, 980–996.

Weckwerth, T.M., Parsons, D.B., Koch, S.E., Moore, J.A., LeMone, M.A., Demoz, B.B., Flamant, C., Geerts, B., Wang, J. and Feltz, W.F. (2004). "An overview of the International H_2O Project (IHOP_2002) and some preliminary highlights". *Bulletin of American Meteorological Society*, 85(2), 253–277.

Weiss, J.L., Gutzler, D.S., Coonrod, J.E.A. and Dahm, C.N. (2004). "Seasonal and inter-annual relationships between vegetation and climate in central New Mexico, USA". *J. Arid Environments*, 57, 507–534.

Zeng, X., Dickinson, R.E., Walker, A. and Shaikh, M. (2000). "Derivation and Evaluation of Global 1-km Fractional Vegetation Cover Data for Land Modeling". *Journal of Applied Meteorology*, 39, 826–839.